CITATION MEASUREMENTS OF CLOUD PROPERTIES DURING CRYSTAL-FACE

Hermann Gerber, Gerber Scientific
Cynthia Twohy, Oregon State U.
Andrew Heymsfield, NCAR
Aaron Bansemer, NCAR
Michael Poellot, U. North Dakota

Abstract

This paper discusses in-situ measurements with aircraft based cloud probes of cloud physical and optical properties during the Crystal-Face (CF) experiment in Florida. Given that the lead author was primarily responsible for the deployment of the CIN (Cloud Integrating Nephelometer) on the Citation aircraft, the subject of this talk will mostly deal with the CIN measurements. The paper is divided into four parts: 1) the CIN is described and related to most of the other cloud probes flown on the Citation as well as the WB-57; 2) an initial attempt is made to compare the cloud probes on the Citation for several case studies ranging from the simplest case, a water cloud with small droplets, to the most complex case, an anvil ice cloud with a broad spectrum of complex crystals; 3) a few examples are given of the extinction coefficient (e) measured by the CIN in anvils, and of the effective radius (Re) given by the ratio of the ice water content (IWC) measured by the counter-flow virtual impactor (CVI), and the particle surface area (PSA) measured by the CIN; and 4) a list of the most significant preliminary observations is given, as well as some recommendations.

The following lists the figures prepared for this presentation. Greater detail of each figure follows this abstract.

Fig. 1 - photo of CIN
Fig. 2 - schematic and capabilities of CIN
Fig. 3 - streamline analysis of flow around CIN
Fig. 4 - cloud-probe size-range comparison
Fig. 5 - scaling FSSP and CIN droplet surface area
Fig. 6 - LWC comparison in warm cloud with small droplets
Fig. 7 - FSSP droplet spectra in warm cloud
Fig. 8 - effective radius (Re) calculations for warm cloud
Fig. 9 - Re comparison in warm cloud
Fig. 10 - CPI images of cloud with large droplets
Fig. 11 - size spectrum of cloud with large droplets
Fig. 12 - Surface area distribution in the overlap region of the CPI and 2-DC probes
Fig. 13 - CPI images of approximately isometric ice crystal aggregates
Fig. 14 - CPI images chain-like aggregates and small particles
Fig. 15 - Comparison of CIN, FSSP, 2-DC extinction coefficients, e, 25 July
Fig. 16 - Comparison of CIN, FSSP, 2-DC extinction coefficients, e, 26 July
Fig. 17 - CPI images of bullet rosettes
Fig. 18 - extinction coefficients (e) measured with CIN, 16 July
Fig. 19 - effective radii (Re) measured with CVI and CIN, 16 July
Fig. 20 - extinction coefficients (e) measured with CIN, 26 July
Fig. 21 - asymmetry parameter (g) measured with CIN, 26 July
Fig. 22 - observations and recommendations
Fig. 23 - questions

FIGURE DETAIL

Fig. 1 - This photograph of the CIN (Cloud integrating Nephelometer) shows an instrument about 60-cm long and weighting 25 lbs. It consists of an electronics enclosure, here seen attached to the underside of an aircraft fuselage; and an elliptical strut that is split down the middle and moved apart about 4 cm forming two separate “wings”. This gap faces into the flight direction of the aircraft, and contains a collimated laser beam (635 nm) that is projected down the center line of the gap. Particles intersecting the laser beam scatter light into detectors imbedded in the inside walls of the wings. For additional information see *Gerber et al., 2000: Nephelometer measurements ..... J. Atmos. Sci., 57, 3021-3034.*

Fig 2 - The CIN measures the asymmetry parameter, g, which is related to the reflectivity of the particles, and which is used to parameterize the scattered light phase function in radiative transfer calculations. It further measures the optical extinction coefficient, e, and the hemispheric backscatter ratio, b. The CIN utilizes four Lambertian detectors (S1 - S4) that measure the light scattered by particles out of the laser beam. This geometry is closely related to one of the integrating nephelometer concepts originally described by *Beutell and Brewer, 1949: Instruments for the measurement of visual range. J. Sci. Instrum., 26, 357-359.* Integrating nephelometers are a well known and proven technology, and they have the advantage of usually containing a relatively large sample volume in comparison to other cloud probes. The “cosine masks” work in conjunction with two of the detectors in order that g can be measured. The CIN produced a continuous data set for all flights of the Citation. On 9 July the CIN data is questionable after 70,000s due to icing conditions.

Fig. 3 - Recently Cynthia Twohy of Oregon State U. utilized fluid dynamic calculations to determine the streamline pattern around the CIN under conditions of 100 m/s aircraft speed, and with the CIN parallel to the aircraft direction. This figure shows the CIN wings and the location of the laser beam looking from the end of the wings. The streamline calculations show only modest deviation from the desired parallel and constant-velocity flow near where particles would intersect the laser beam. The flow initially decelerates in front of the wings, but has close to the free air velocity in between the wings. There is however, some shear noticeably near the front of the wings and the center axis, suggesting that oriented ice crystals may change orientation as a result.

Fig. 4 - In order to illustrate how the CIN relates to the other cloud probes, the estimated size range of operation of most of the cloud probes used during C-F is compared. The probes fit into two categories; the first are “single-particle” probes that measure the image or signal from individual particles to generate a size spectrum, and the second are “integral” probes that sense an ensemble of particles and directly measure an integrated property of the size spectrum. For the latter, the CIN measures the 2d moment (particle surface area or e) of the spectrum, while the CVI measures the 3d moment (volume of the condensed phase).

It was suggested earlier by Brian Toon, as well as other speakers at this meeting that the data from the two categories of probes should be compared. There are several reasons why this suggestion makes sense: 1) the most obvious reason is that the integral probes cover a particle size range that encompasses nearly the entire range of interest; whereas, the single particle probes only cover increments of this range, and thus data must be combined from several probes to cover the entire range; 2) the sample volume of the integral probes is generally much greater and easier to define than that of the single-particle probes, potentially

making measurements with the former easier to make; 3) the output of the single-particle probes depends on particle shape; whereas, the output of the integral probes does not; and 4) data from all the probes listed in this figure are directly comparable.

It has been clear from the literature for some time that the single-particle probes generally produce data with large error bars, especially when integrated properties are derived from particle spectra. The possibility exists to constrain the errors in those probes by scaling their outputs to the outputs of the integral probes, if the latter are considered as producing accurate results. This procedure could be best applied to clouds with spherical particles; application to clouds with ice particles would be more difficult given the various ways single-particle probes are used to sense ice crystals.

Fig. 5 - A comparison is shown of droplet surface area measured with the CIN and FSSP while flying horizontally with the NCAR C-130 in a stratocumulus during the recent DYCOMS-II study. This illustrates that scaling the FSSP measurements with a constant value can yield close agreement with the CIN.

Fig. 6 - Fig. 9 - This series of figures compares the King, CVI, FSSP, and CIN probes on the Citation for the simplest cloud scenario: a warm cloud with droplet sizes that all fall within the size ranges for these probes. Figure 6 shows LWC measured by three of the probes over a period of about 20s; significant differences are seen. Figure 7 shows all the size spectra for the 20-s period; the lines connect only the spectra points for 65,479s and 65,480s seen in Fig. 6. The CIN measurement of e (or particle surface area) can be compared to the preceding three probes by comparing Re as calculated in Fig. 8. The results of this comparison are shown in Fig. 9, and raise the possibility that the CIN was making accurate measurements, given that the scaling of the FSSP is likely not an issue here, and that the relative shape of the FSSP spectra have been though to be reasonably accurate. However, this single result is not definitive proof of CIN accuracy, nor does it disqualify the King probe or CVI measurements from being more accurate. Unfortunately, the Citation did not fly through additional warm clouds during C-F with all probes functioning, so that this approach can not be expanded.

Fig. 10 - Fig. 12 - This series of figures looks at probe performance for a droplet cloud with increased complexity, where large drops (an a few ice crystals) extend into the size range of the 2-DC and CPI probes. Figure 10 shows CPI images of drops in this cloud; the arrow in the upper left indicates that the largest drops are about 200-um in diameter. The value of g (.860) measured by the CIN is close to what one would expect from Mie calculations for these drops. Figure 11 compares FSSP, CPI, and 2-DC spectra for this cloud; agreement is poor with significant roll off in the latter two probes for particles smaller than 50 um - 100 um. Figure 12 magnifies the spectral region where the 2-DC and CPI probes overlap, and shows the droplet area measured by each. The difference in the surface area measured by the two probes in the overlap region averages a factor of 3.

Fig. 13 - This CPI image shows ice particles with increased complexity. These ice particles are reasonably isometric and consist mostly of tightly packed aggregates. Probe comparisons for this case are yet to be made. This type of particle produced the smallest values of g, some values being smaller than .700.

Fig. 14 - This CPI image shows ice particles with a high degree of complexity. Some particles appear to consist of chain-like aggregates, while others appear like small frozen droplets. This case is from an anvil outflow with the Citation flying at a highest level.

Fig. 15 - Fig. 16 - The extinction coefficient, e, measured directly with the CIN is compared to a calculated e from spectra measured with the 2-DC and FSSP for the entire Citation flight on July 25 (Fig. 15), and for July 26 (Fig. 16). The correlation between the measurements is remarkably good, suggesting that the treatment of the anvils' wide variety of complex ice crystals in calculating e from spectra is consistent. There is, however, about a factor of 2 offset between CIN and 2-DC + FSSP e measurements, which also appears in the rest of the entire Citation data set. As of now no explanation has been found as to the reason behind this factor of 2 offset.

The few preceding descriptions of probe comparisons illustrate again the difficulty of obtaining consistency among cloud probes, especially when higher moments of the spectra are calculated. This should not lower one's opinion of single-particle probes, given that only they can give particle shape and size information which is crucial for physical process studies that feed models. However, when properties such as LWC, IWC, extinction, and optical thickness are needed, the integral probes should be used, or an attempt made to scale the single-particle probes to the integral probes (assuming that the latter can be trusted). In any case, the two types of probes should be flown together on the same aircraft whenever possible, given the potential synergisms between the two types.

Fig 17 - The last CPI image shows bullet rosettes observed on Citation flight on 25 July. This is a rare instance in the entire Citation ice-crystal data set where well-defined single crystal shapes were present. These crystals produced a relatively large value of g. The CPI data set from the Citation shows that anvils and associated clouds in C-F consisted of ice particles for which the large majority could be classified as "junk ice", with a wide range of different aggregates, other complex shapes, and wide spectral ranges, reflecting perhaps the high degree of turbulence and mixing in the Florida storms. Small frozen droplets also were prevalent at high levels.

Fig 18 - This figure is an example of the extinction coefficient, e, data produced by the CIN during C-F; this is for the Citation flight on 16 July. Profiles through two anvils are shown by 1 and 2. The former corresponds to an upward aircraft spiral though an aged anvil near the western ground site, while the latter corresponds to transects at ever lower altitudes of a new anvil. Generally, e increases with high in the anvils; however, the aged anvil shown by 1 has the opposite trend. The dense anvil cloud indicated by 2 is at the highest level flown by the Citation and closest to the anvil source region, and contains many small crystals and their aggregates as shown in Fig. 14 which corresponds to 2 in the present figure.

Fig. 19 - The effective radius, Re, calculated by ratioing the CVI (IWC) and CIN (e) measurements is shown for the 16-July flight. The general decrease of Re with increasing height in the anvils as shown by 1 and 3 is consistent with the trend seen in the rest of the Re data set. The smallest values of Re of about 10 um are found at the highest anvil level 2 and are consistent with the small crystals and their aggregates seen by the CPI.

Fig. 20 - Fig. 21 - A second example of extinction measured by the CIN on 26 July is shown in Fig. 20. Here the Citation spiraled down through a cloud three times for the "melting layer experiment". Figure 21 magnifies the time interval for the central spiral and shows values of g as the aircraft descended incloud from a temperature of -10 C to +10 C. The pass through the 0 C isotherm is highly correlated with an increase in g, and the pass through a cloud portion with only water droplets yields close to the expected value of g. The values of g close to .890 correspond to regions with rain.

Fig. 22 - The reduction of the CIN data, and initial data analysis of this data and of other Citation cloud probes has led to the following **observations**:

1) The Florida thunderstorms contain regions that are exceptionally dense optically, with large values of the extinction coefficient. These “extinction core” regions appear to be located with and a result of updraft cores.

2) The average ice-crystal size in the anvils, as indicated by Re, invariably decreases with height, as has been noted also in earlier studies by A. Heymsfield.

3) The extinction coefficient increases with height in the anvils in most cases, except perhaps close to anvil top.

4) The CIN on the Citation produced a rich data set of g values which will be related in subsequent analyses to various cloud and environmental parameters. The value of g in the anvils varies over a relatively small value about .730. This value is close to the average value of g measured by the CIN instrument in Arctic ice clouds during the SHEBA-FIRE study (*Garrett et al, 2001: Shortwave, single-scattering ..... J. Geophys. Res., 106, 15,155-15,172*). The largest values of g in the Florida clouds correspond to pristine single-habit crystals and to small frozen droplets and their low-density aggregates, while the smallest values of g, some smaller than .700 correspond to dense aggregates.

5) The value of g is sensitive to the ratio of water to ice in the clouds. The measurement of g provides a quick indication of cloud composition without having to look at data from particle imaging probes.

6) The cloud probes on the Citation showed significant disagreement when integrated properties of the cloud particles, such as LWC and extinction, were compared.

Two **recommendations** are given in this figure:

1) The first suggests additional aircraft flights in water and ice clouds focused on better defining accuracy and synergism between cloud probes. In particular, a formal strategy should be evolved that stresses the optimum relationship between “single-particle” and “integral” probes. This would include specifying different cloud-types to fly through in order to enhance accuracy of given probes of the probe ensemble. A simple example would consist of flying through small-droplet warm clouds for improving scaling accuracy of the FSSP.

2) CIN scaling accuracy depends on co-located comparisons with the surface area channel of the PVM (Particle Volume Monitor) in a cloud chamber. A more direct calibration of the CIN is recommended. This could be in the form of a monodisperse glass-bead sedimentation chamber or transmissometer run co-located with the CIN in an ambient cloud environment.

Fig. 23 - The answer (in the opinion of the principal author) to the first question would be “in most cases the accuracy of the cloud probes is insufficient”. While in some cases, such as narrow size distributions of cloud particles, the relative size spectrum can be quite accurate; however, the broader spectra measured by an ensemble of different probes rarely matches up. When integrated properties calculated from the spectra are desired the accuracy decreases further. Integral probes can improve the overall lack of accuracy, if they themselves can be proved to be accurate.

Calibration of cloud probes is often an individual matter. A national facility to calibrate the probes would be beneficial. The two icing tunnels (NASA Lewis and NRC of Canada) that have been used for calibrations are not designed specifically for probe calibration. Innovative and improved means to generate drops and ice crystals more realistic as to what is found in ambient clouds would need to be part of a national facility.

Fig. 1

CLOUD INTEGRATING NEPHELOMETER
(g-meter)

1. asymmetry parameter, g
2. optical extinction coefficient
3. backscatter ratio

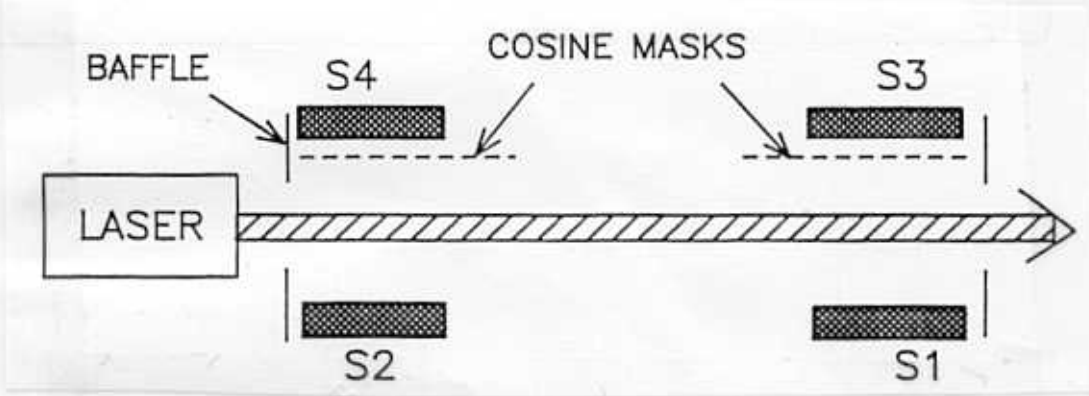

Fig-2

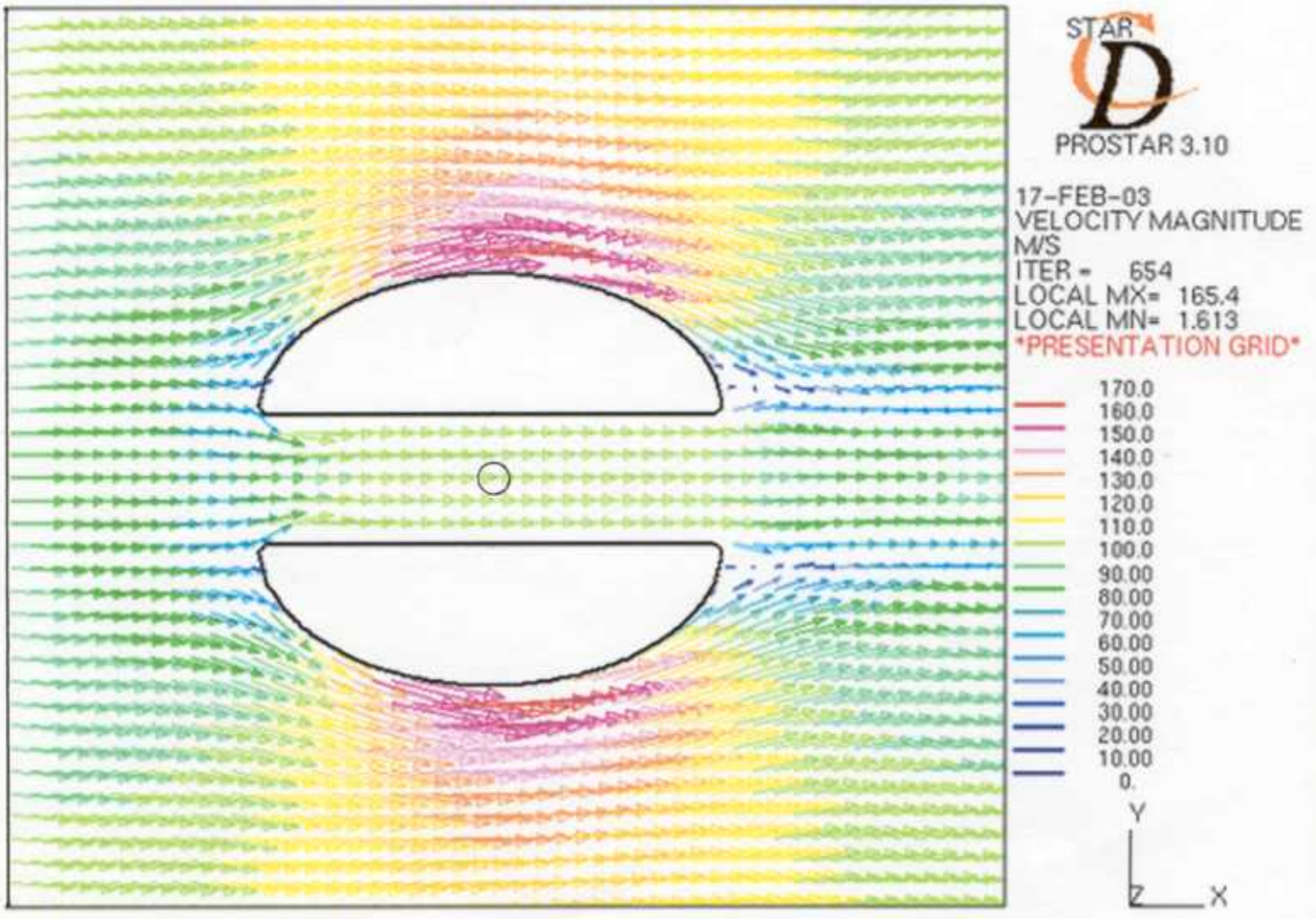
STAR
PROSTAR 3.10
17-FEB-03
VELOCITY MAGNITUDE
M/S
ITER = 654
LOCAL MX= 165.4
LOCAL MN= 1.613
PRESENTATION GRID
170.0
160.0
150.0
140.0
130.0
120.0
110.0
100.0
90.00
80.00
70.00
60.00
50.00
40.00
30.00
20.00
10.00
0.
Y
Z
X

Fig. 3

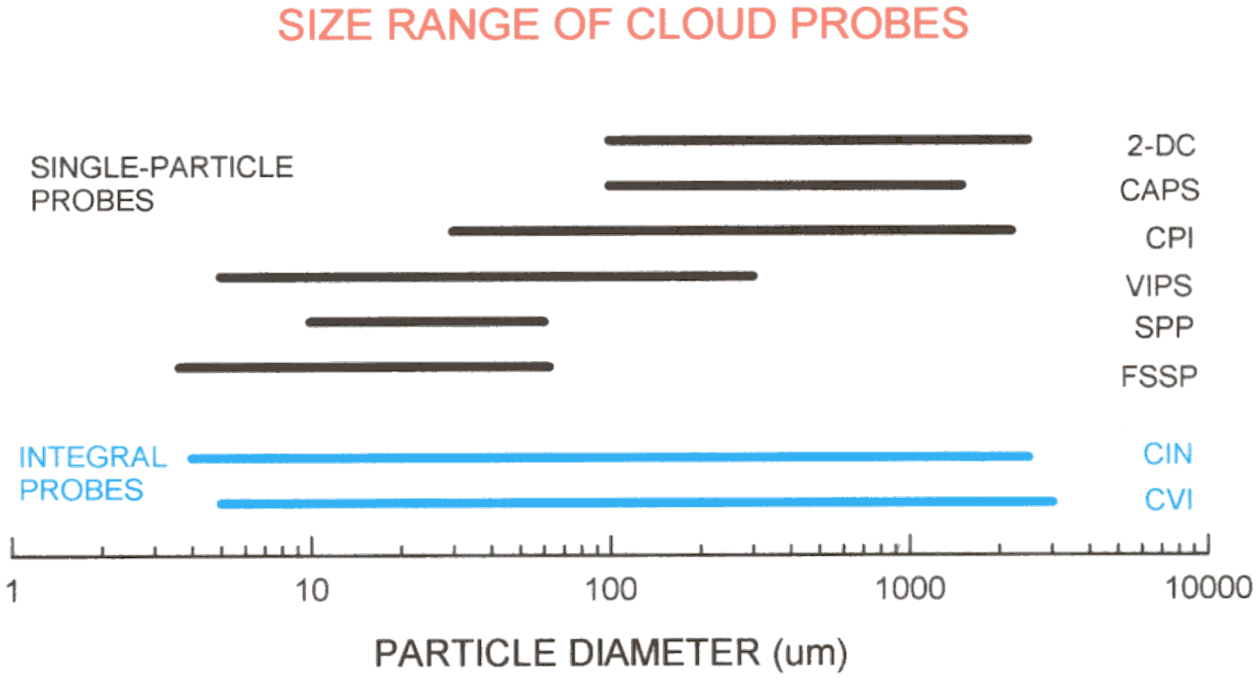

	SAMPLE VOLUME	DEPEND ON PARTICLE SHAPE	DIRECT COMPARISON
SINGLE-PARTICLE PROBES	tiny	yes	yes
INTEGRAL PROBES	large	no	yes

Fig. 4

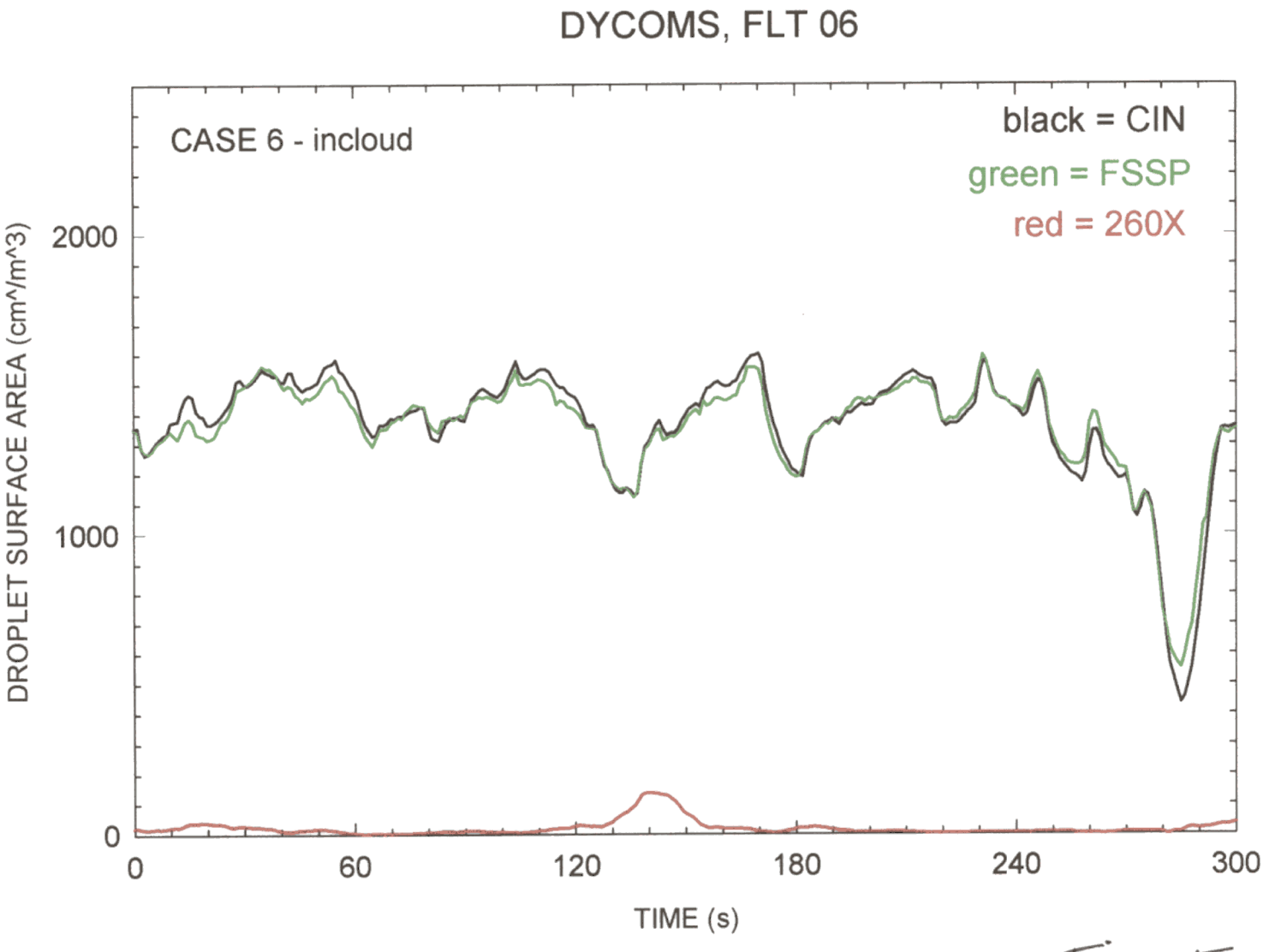
DYCOMS, FLT 06
CASE 6 - incloud
black = CIN
green = FSSP
red = 260X
DROPLET SURFACE AREA (cm^/m^3)
2000
1000
0
0
60
120
180
240
300
TIME (s)

Fig. 5

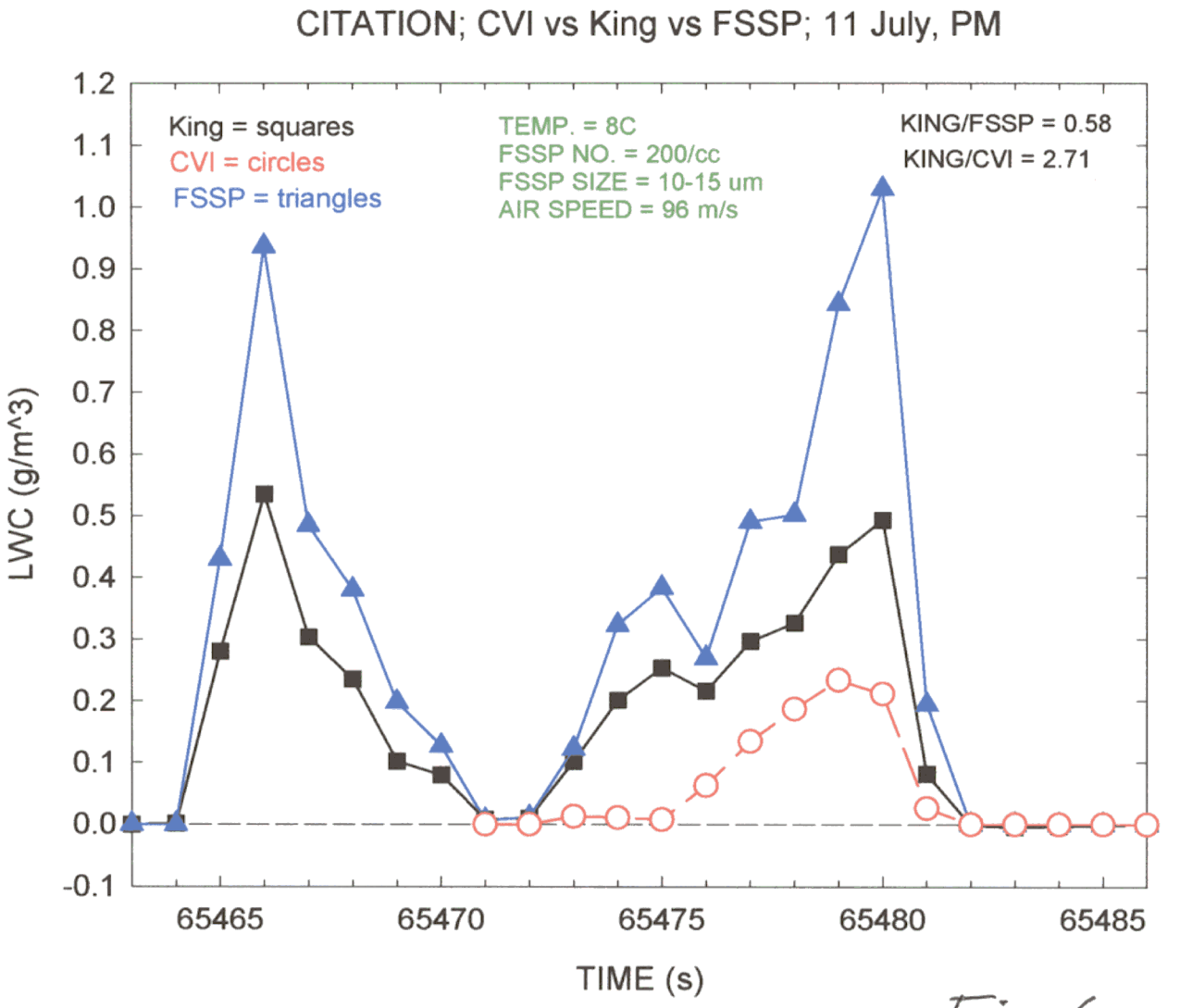
CITATION; CVI vs King vs FSSP; 11 July, PM
King = squares
CVI = circles
FSSP = triangles
TEMP. = 8C
FSSP NO. = 200/cc
FSSP SIZE = 10-15 um
AIR SPEED = 96 m/s
KING/FSSP = 0.58
KING/CVI = 2.71
LWC (g/m^3)
1.2
1.1
1.0
0.9
0.8
0.7
0.6
0.5
0.4
0.3
0.2
0.1
0.0
-0.1
65465
65470
65475
65480
65485
TIME (s)

Fig. 6

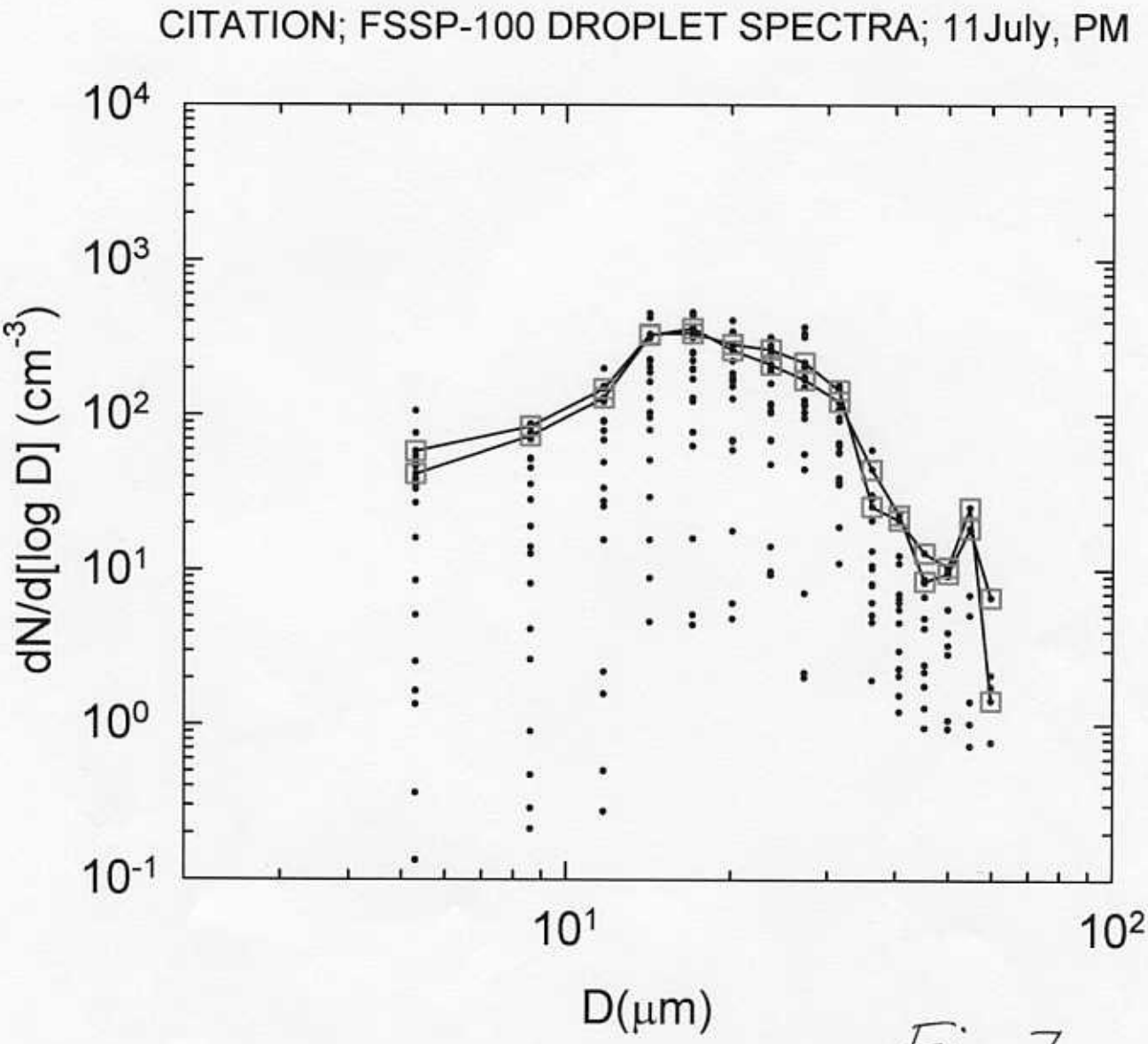
CITATION; FSSP-100 DROPLET SPECTRA; 11July, PM
dN/d[log D] (cm-3)
10^4
10^3
10^2
10^1
10^0
10^-1
10^1
10^2
D(μm)

Fig. 7

EFFECTIVE RADIUS

$$R_e = \sum_r \frac{r^3 n(r) \Delta r}{r^2 n(r) \Delta r}$$

FSSP $$R_e = C \frac{FSSP\,(VOLUME)}{FSSP\,(AREA)} = 11.7\ \mu m$$

CIN $$R_e = C \frac{FSSP\,(VOLUME)}{CIN\,(EXT.\ COEFF.)} = 11.4 \mu m$$

KING $$R_e = C \frac{KING\,(VOLUME)}{CIN\,(EXT.\ COEFF.)} = 6.6 \mu m$$

CVI $$R_e = C \frac{CVI\,(VOLUME)}{CIN\,(EXT.\ COEFF.)} = 2.4 \mu m$$

Fig. 8

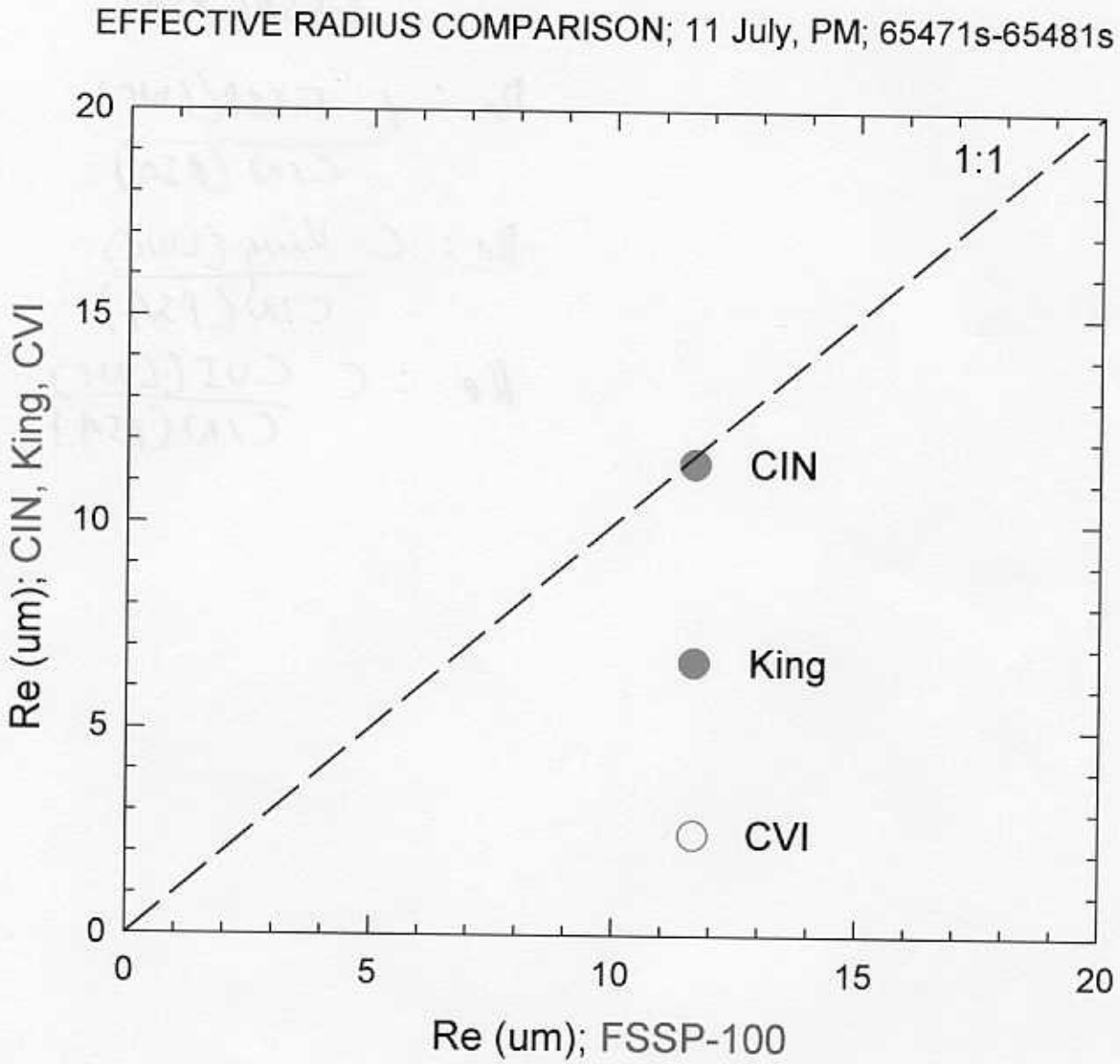
EFFECTIVE RADIUS COMPARISON; 11 July, PM; 65471s-65481s
20
15
10
5
0
0
5
10
15
20
1:1
CIN
King
CVI
Re (um); CIN, King, CVI
Re (um); FSSP-100

Fig. 9

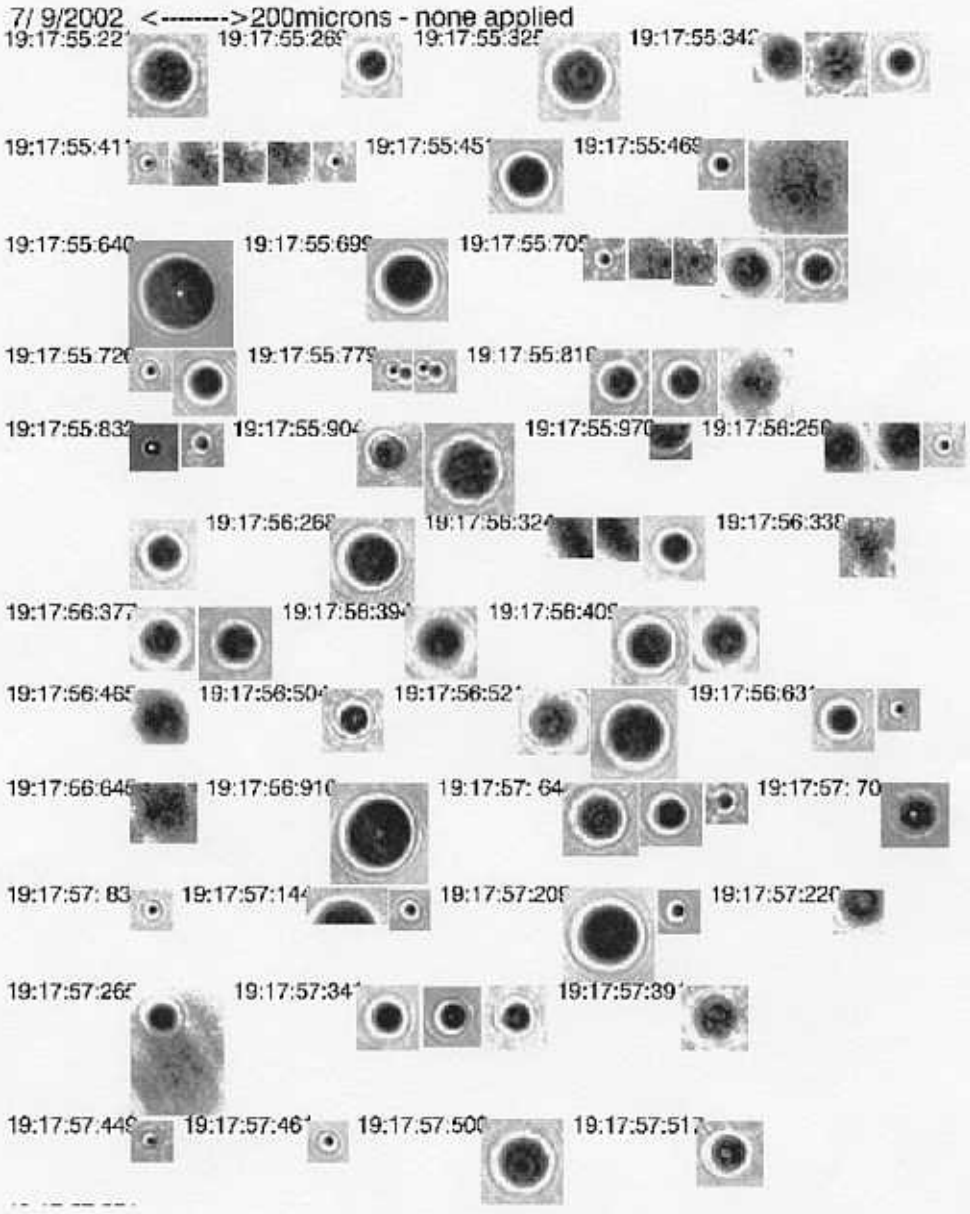

g =.860 +/-.024

T = -5 C
H = 5,500 m

Fig. 10

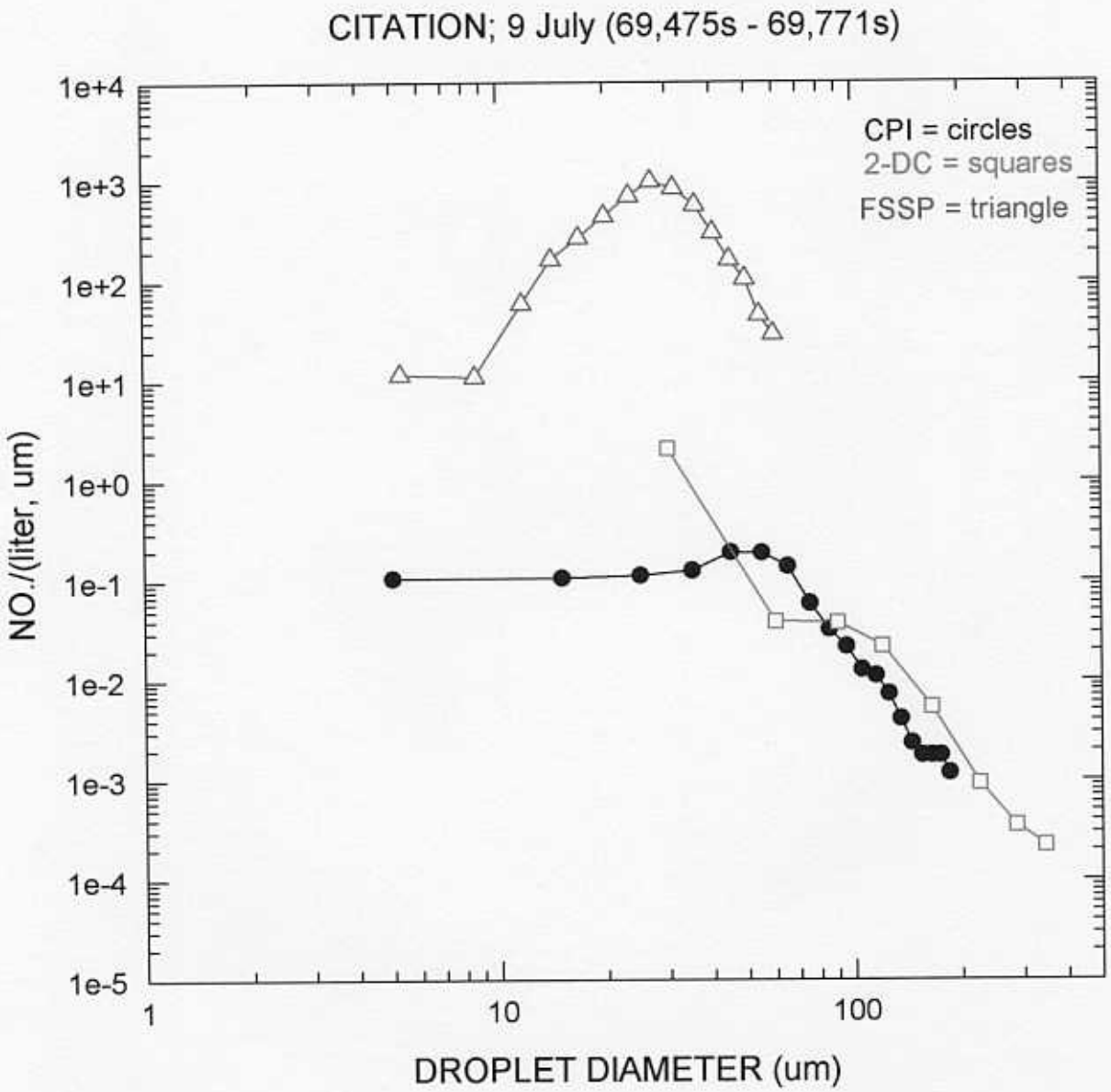
CITATION; 9 July (69,475s - 69,771s)
CPI = circles
2-DC = squares
FSSP = triangle
NO./(liter, um)
1e+4
1e+3
1e+2
1e+1
1e+0
1e-1
1e-2
1e-3
1e-4
1e-5
1
10
100
DROPLET DIAMETER (um)

Fig. 11

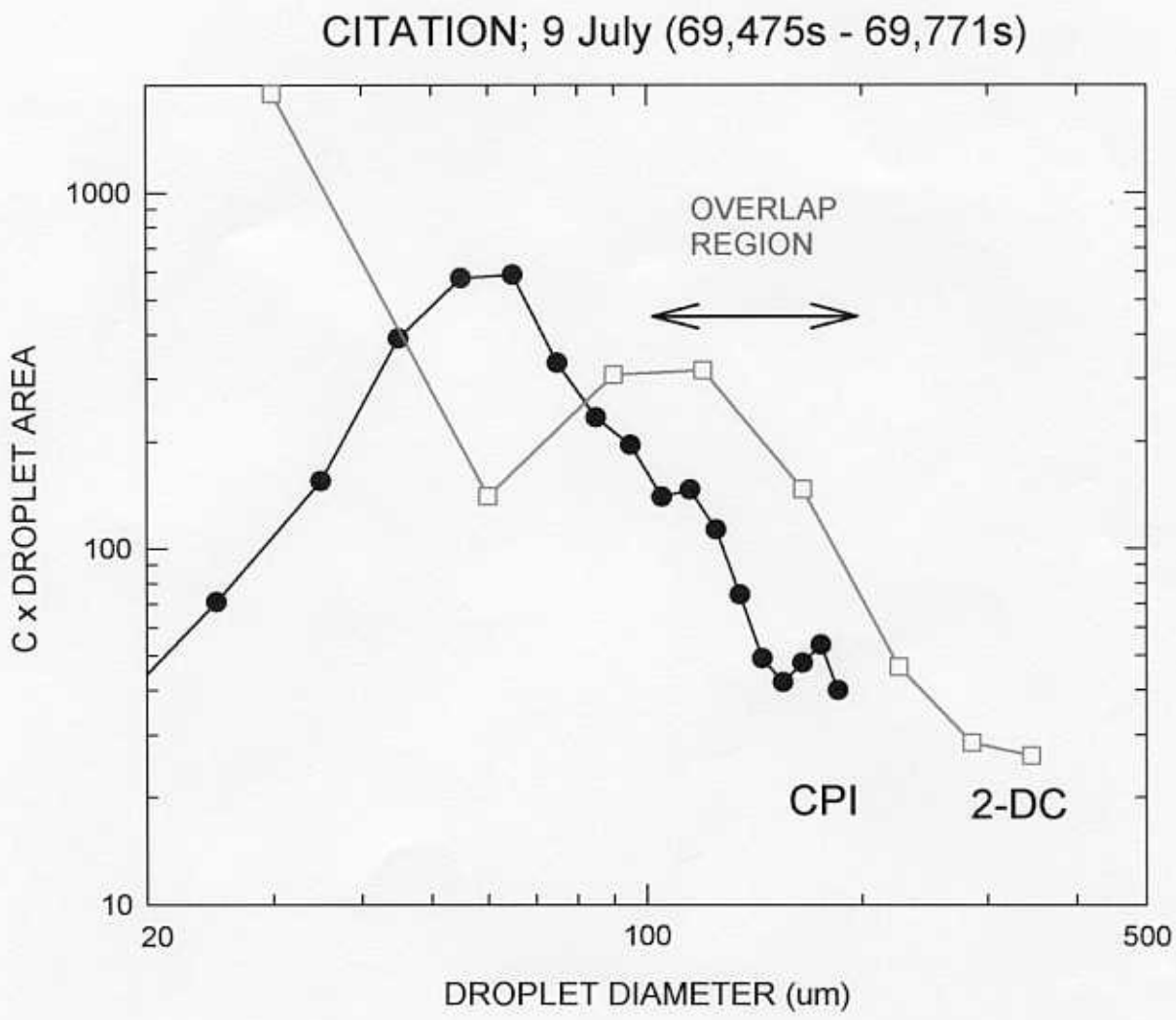
CITATION; 9 July (69,475s - 69,771s)
1000
100
10
C x DROPLET AREA
OVERLAP
REGION
CPI
2-DC
20
100
500
DROPLET DIAMETER (um)

Fig. 12

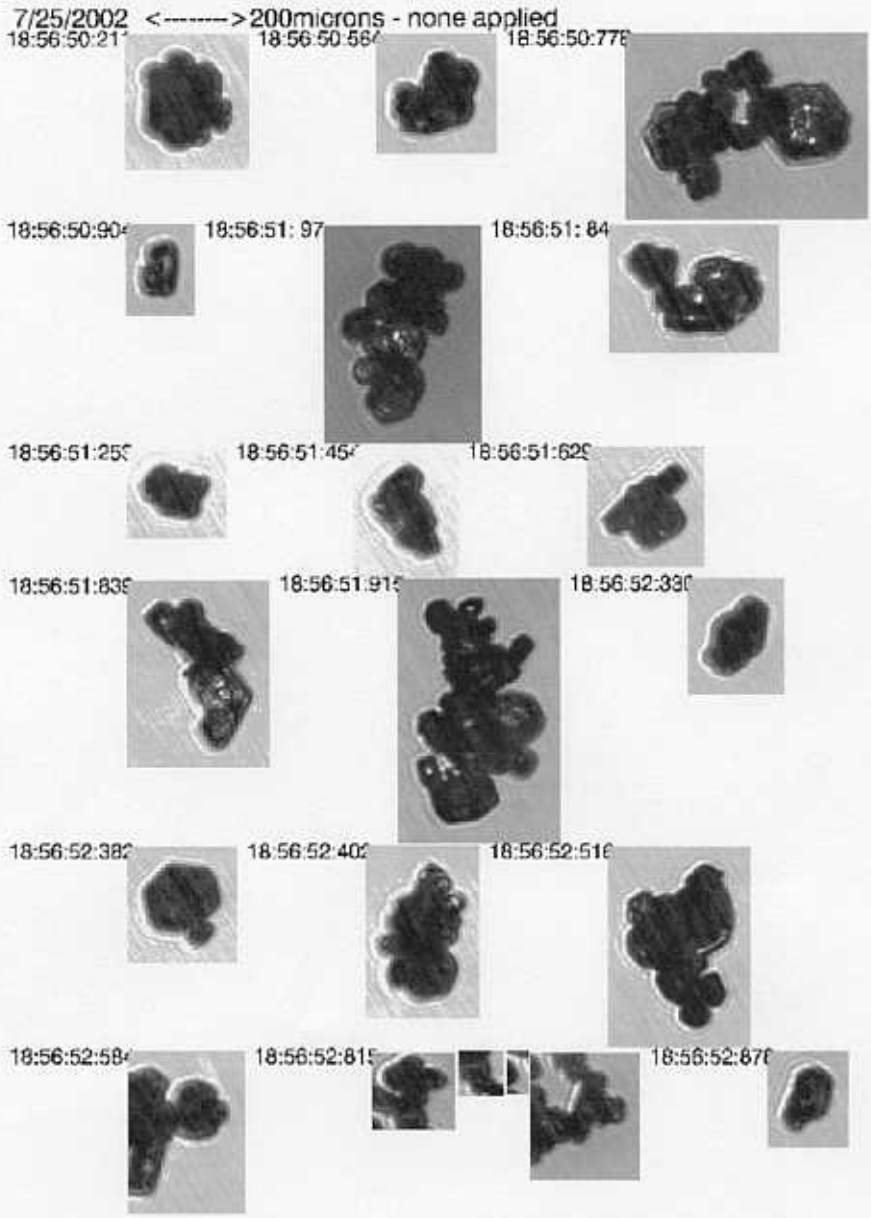

g = .681 +/- .013

T = -38 C
H = 10,000 m

Fig. 13

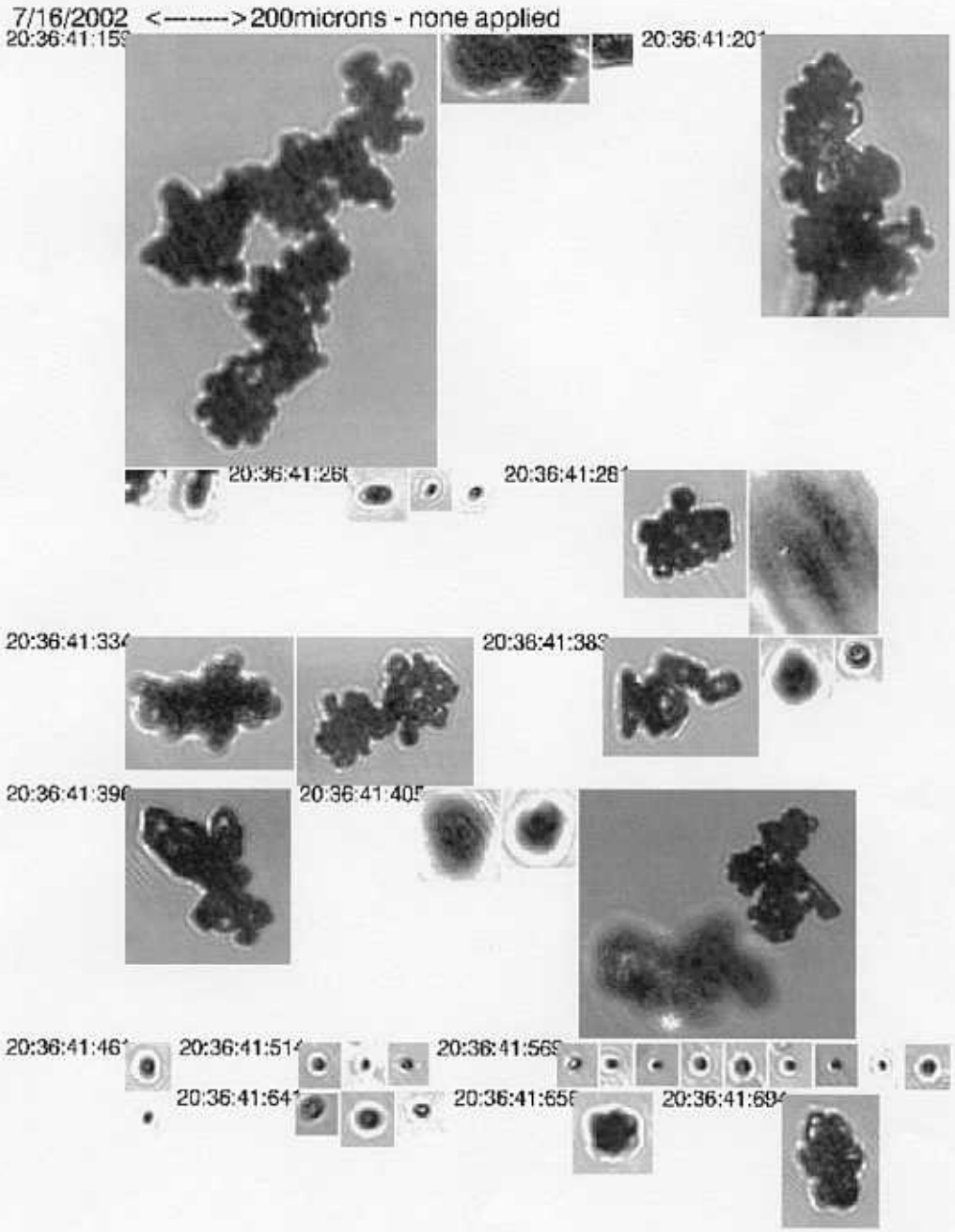

g = .737 +/- .006

T = -49 C
H = 12,000 m

Fig. 14

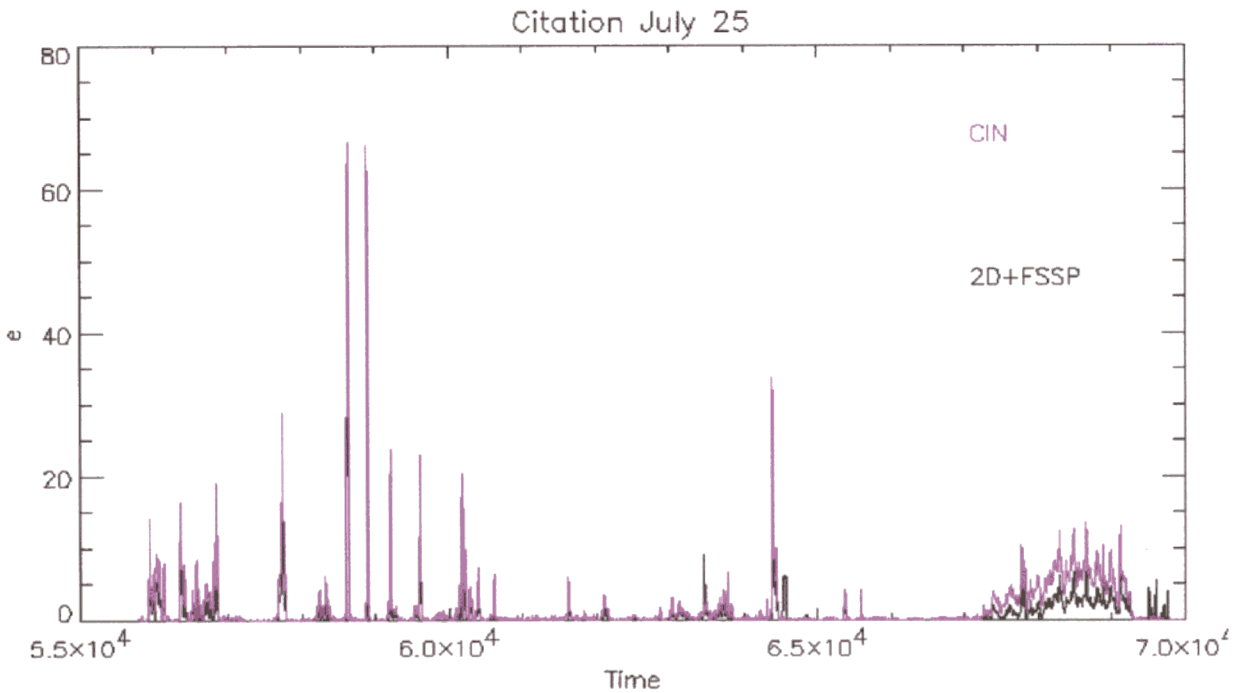
Citation July 25
CIN
2D+FSSP
e
Time
80
60
40
20
0
5.5x10^4
6.0x10^4
6.5x10^4
7.0x10^4

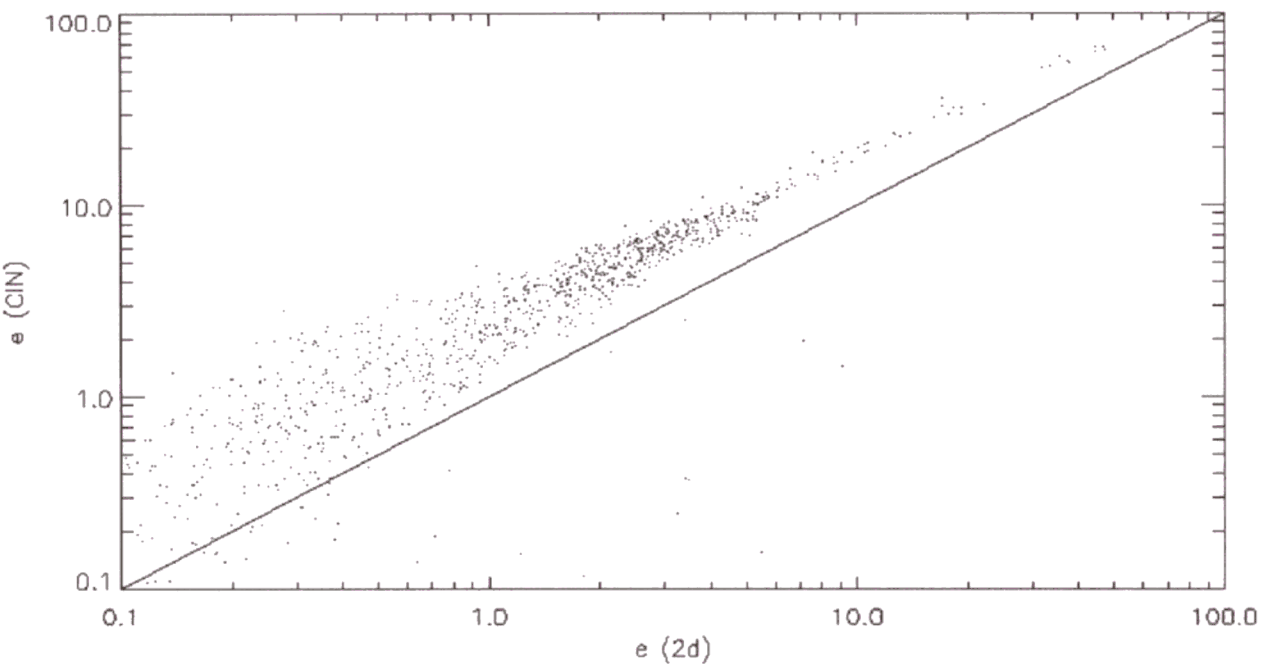
e (CIN)
e (2d)
100.0
10.0
1.0
0.1
0.1
1.0
10.0
100.0

Fig. 15

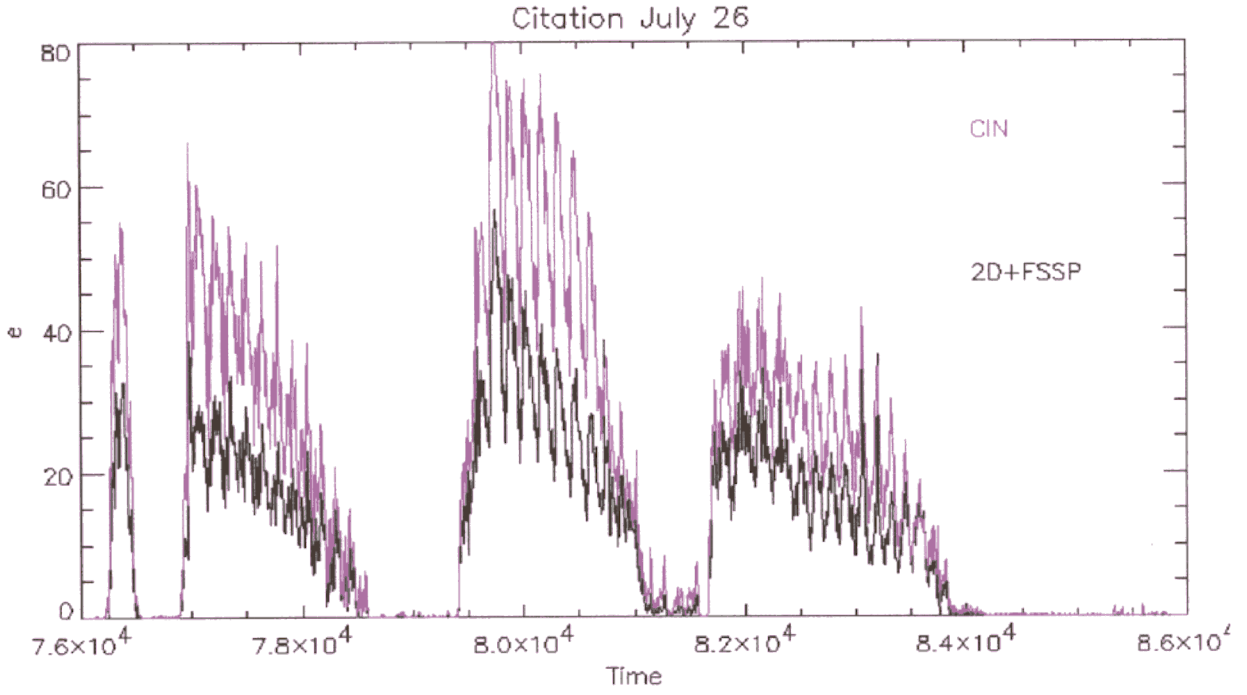
Citation July 26
CIN
2D+FSSP
e
Time
80
60
40
20
0
7.6x10^4
7.8x10^4
8.0x10^4
8.2x10^4
8.4x10^4
8.6x10^4

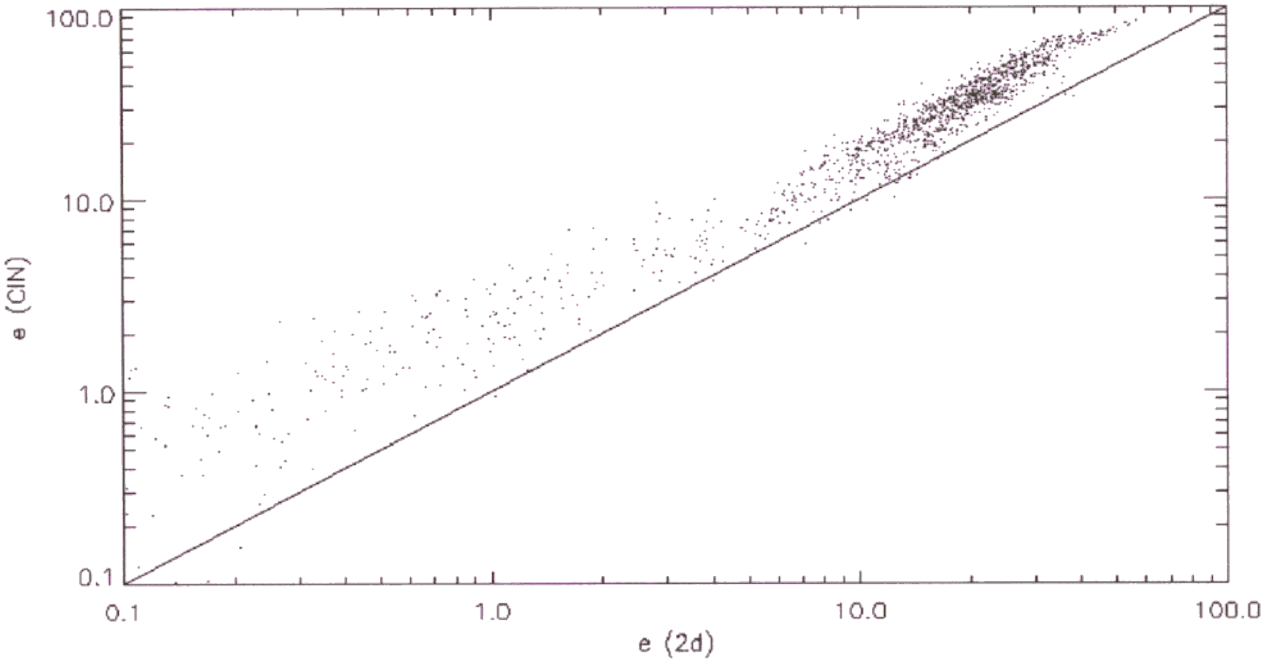
e (CIN)
e (2d)
100.0
10.0
1.0
0.1
0.1
1.0
10.0
100.0

Fig. 16

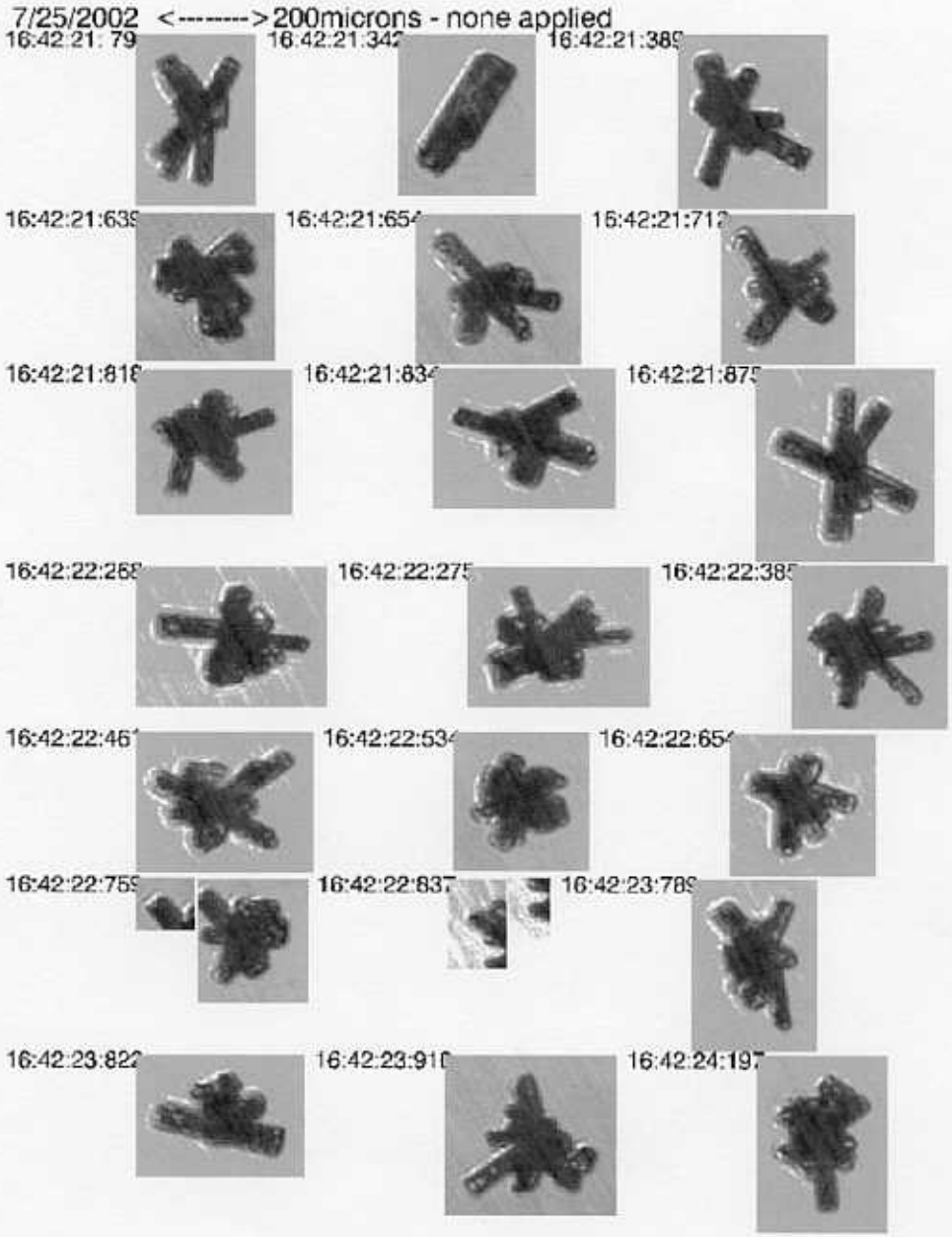

g = .757 +/- .007

T = - 46 C
H = 10,400 m

Fig. 17

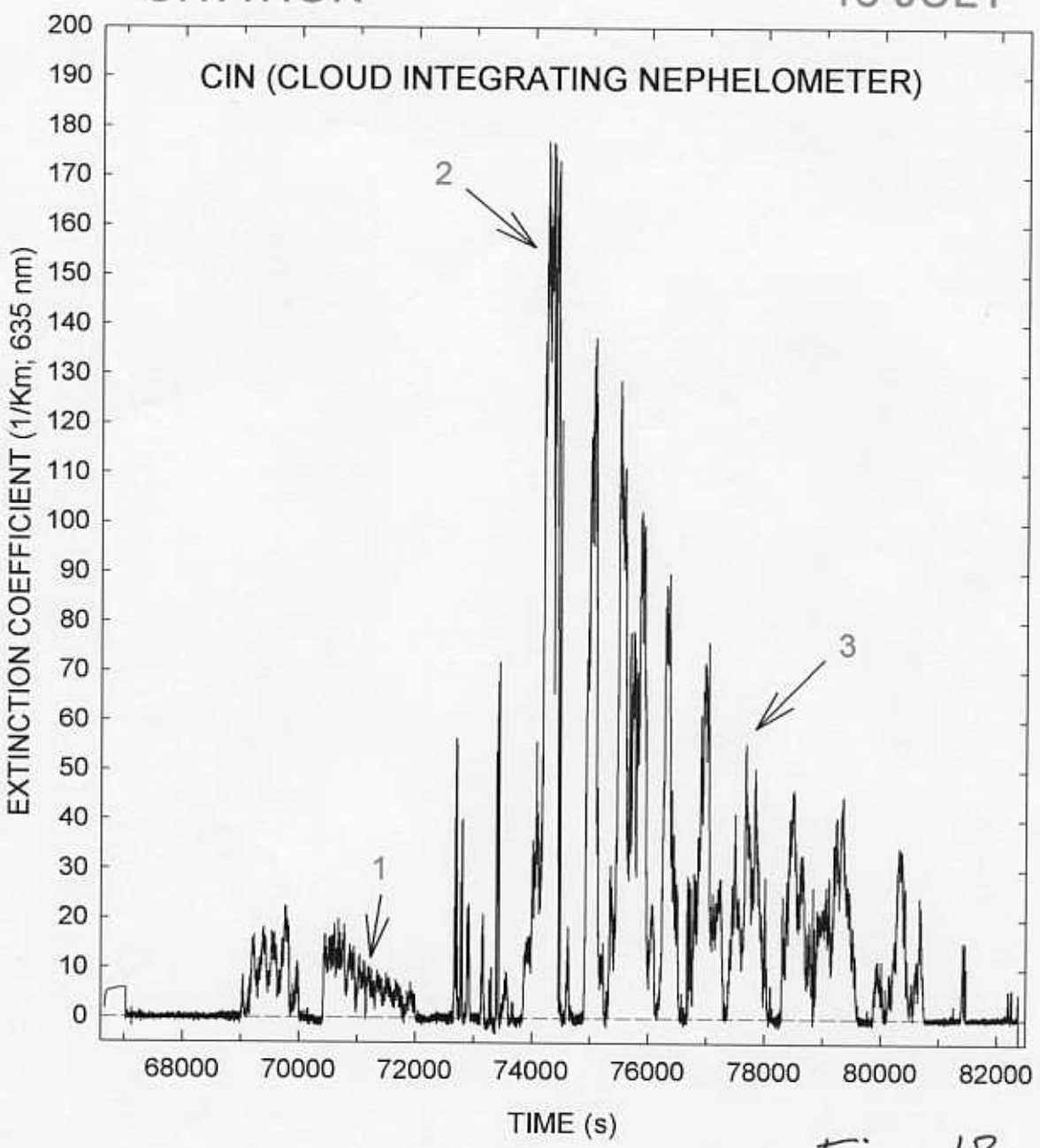
CITATION
16 JULY
CIN (CLOUD INTEGRATING NEPHELOMETER)
EXTINCTION COEFFICIENT (1/Km; 635 nm)
TIME (s)
1
2
3
200
190
180
170
160
150
140
130
120
110
100
90
80
70
60
50
40
30
20
10
0
68000
70000
72000
74000
76000
78000
80000
82000

Fig. 18

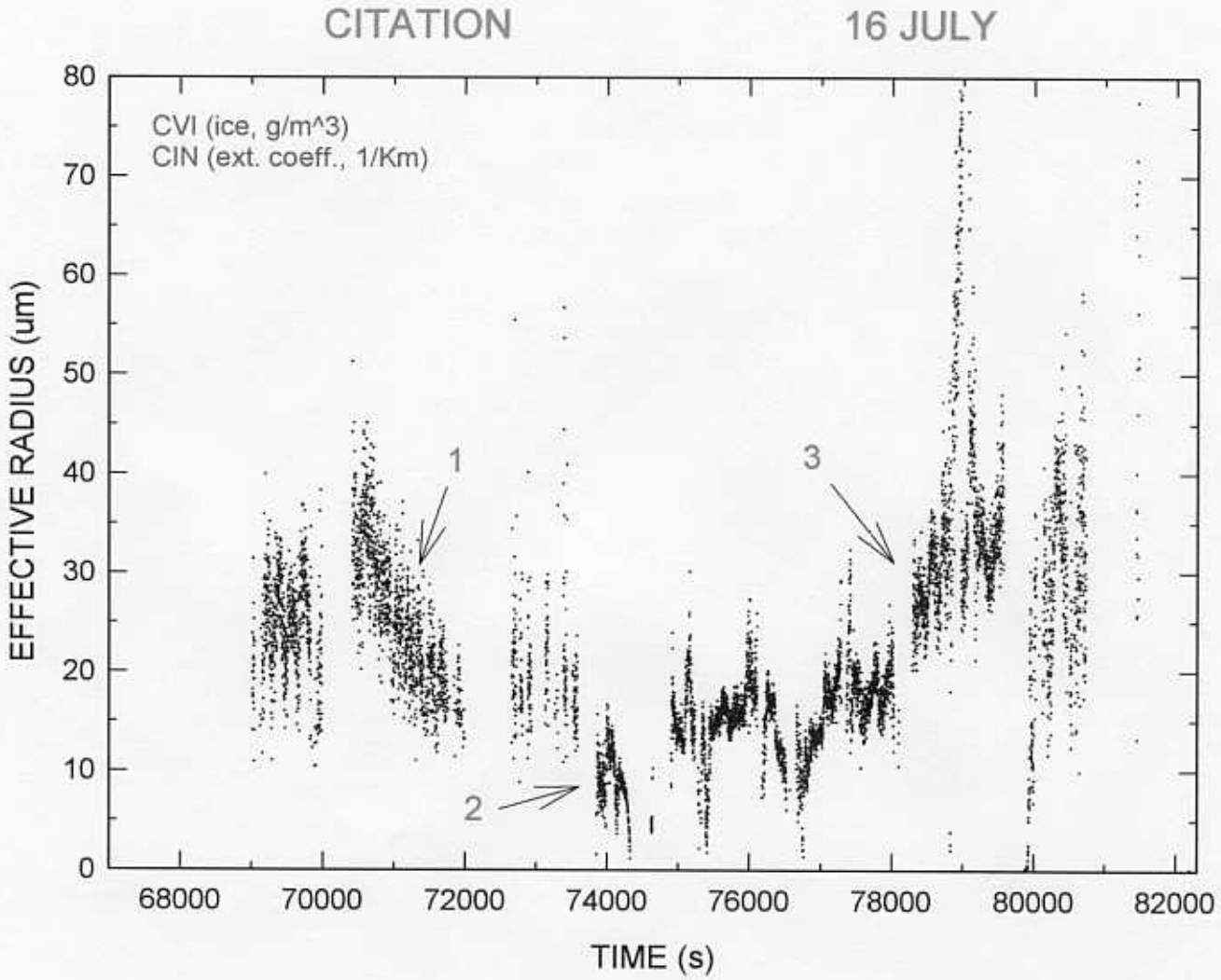
CITATION
16 JULY
CVI (ice, g/m^3)
CIN (ext. coeff., 1/Km)
EFFECTIVE RADIUS (um)
TIME (s)
0
10
20
30
40
50
60
70
80
68000
70000
72000
74000
76000
78000
80000
82000
1
2
3

Fig. 19

CITATION 26 JULY

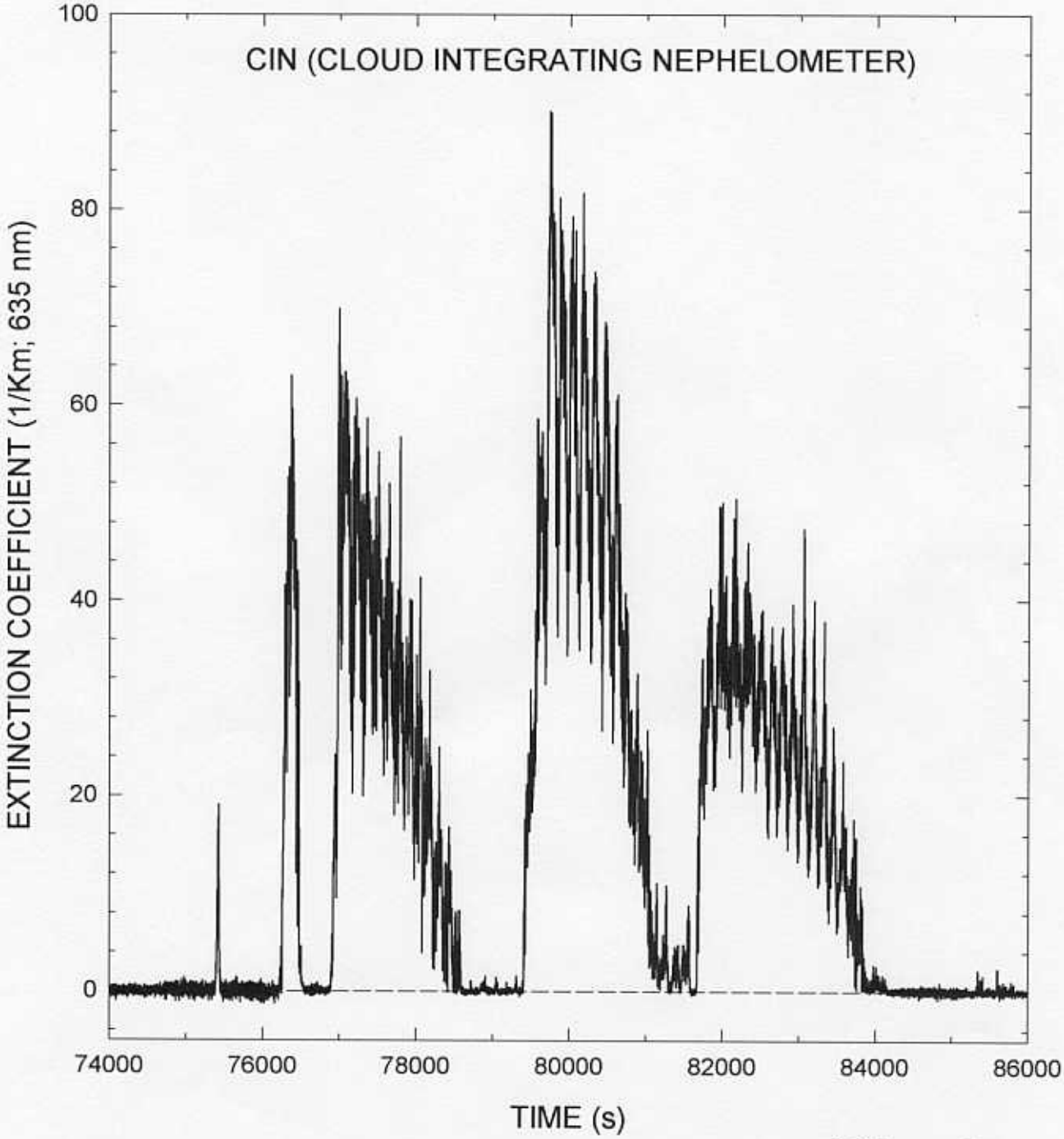

Fig. 20

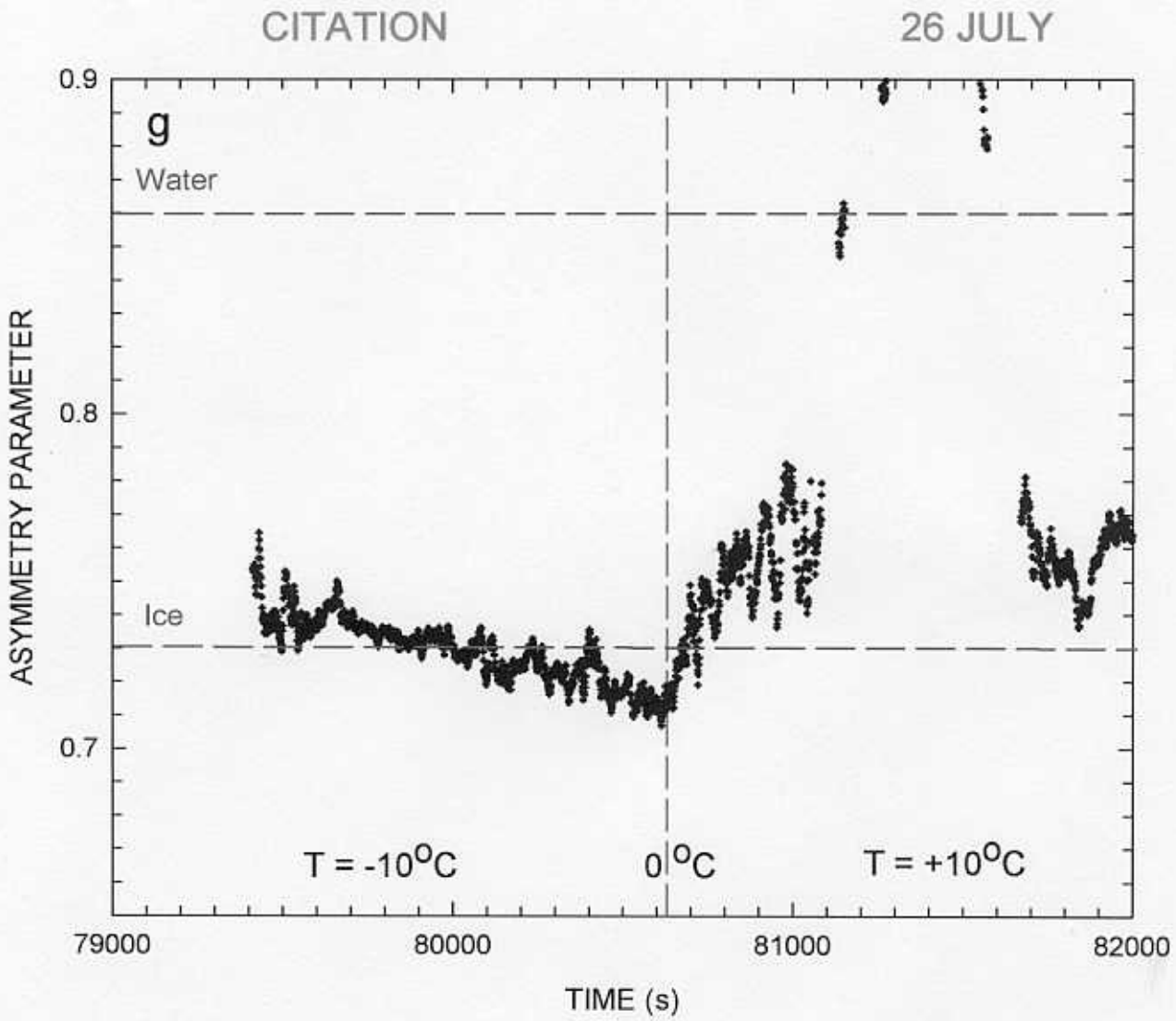
CITATION
26 JULY
g
Water
Ice
0.9
0.8
0.7
ASYMMETRY PARAMETER
T = -10°C
0 °C
T = +10°C
79000
80000
81000
82000
TIME (s)

Fig. 21

OBSERVATIONS

1. Existence of "extinction cores" with many small particles
2. Particle size, Re, decreases with height
3. Ext. coeff. increases with height (except near cloud top?)
4. g in ice varies over a small range around .73
5. g indicates ice or water presence and mixture thereof
6. Cloud probes disagree

RECOMMENDATIONS

1. Additional Citation flights in warm, mixed phase, and ice clouds with FSSP, 2-DC, CPI, CVI, CIN, PVM, and King probes focussed on probe accuracy and synergism.
2. Design/construct glass-bead sedimentation chamber for CIN

Fig. 22

ARE CLOUD PROBES SUFFICIENTLY ACCURATE TO SERVE AS "GROUND TRUTH" FOR REMOTE SENSING?

A NATIONAL CALIBRATION FACILITY FOR CLOUD PROBES?

Fig. 23